$\eta, \eta' \to \pi^+\pi^-\gamma$ with coupled channels

B. Borasoy[1], R. Nißler[2]

Physik Department
Technische Universität München
D-85747 Garching, Germany

Abstract

The decays $\eta, \eta' \to \pi^+\pi^-\gamma$ are investigated within an approach that combines one-loop chiral perturbation theory with a coupled channel Bethe-Salpeter equation which satisfies unitarity constraints and generates vector mesons dynamically from composite states of two pseudoscalar mesons. It is furthermore shown that the inclusion of the η' as a dynamical degree of freedom does not renormalize the Wess-Zumino-Witten term.

PACS: 12.39.Fe

Keywords: Chiral Lagrangians, anomaly, unitarity.

[1]email: borasoy@ph.tum.de
[2]email: rnissler@ph.tum.de

1 Introduction

The decay $\eta \to \pi^+\pi^-\gamma$ is determined entirely by the chiral anomaly, if the quark masses of the up, down and strange quarks and the involved four-momenta are sent to zero. The kinematical region of the decay, on the other hand, is constrained to $4m_\pi^2 \leq (p^+ + p^-)^2 \leq m_\eta^2$ with p^+ and p^- the four-momenta of the π^+ and π^-, respectively, and thus far from the zero momentum limit which is described by the anomalous Wess-Zumino-Witten (WZW) term in the chiral effective Lagrangian [1, 2].

In the framework of chiral effective field theory higher order contact interactions as well as unitarity corrections which arise from loop graphs will be of importance and must be included in order to enable a proper description of the experimental decay width and the photon spectrum, see, *e.g.*, [3] for a one-loop calculation and [4, 5] for experimental results.

For the decay $\eta' \to \pi^+\pi^-\gamma$ contributions from vector meson exchange will dominate the amplitude and unitarity effects should be implemented via final state interactions. This is clearly beyond the perturbative framework of chiral perturbation theory (ChPT) and requires utilization of non-perturbative tools which match onto the results from ChPT. One obvious approach would be to employ the vector dominance picture with energy-dependent widths in the vector meson propagators. However, this procedure can be shown to be in contradiction to the one-loop result of ChPT [6].

Another possibility is to postulate an N/D structure for the decay amplitude which matches onto both the one-loop chiral corrections and vector meson dominance in the pertinent limits. This approach has been applied successfully in [7], where the decay width and photon spectra of both the η and η' decay are brought to agreement with experiment [8, 9] and constraints for the η-η' mixing angle have been given.

In the present investigation we will apply an alternative approach which relies solely on chiral symmetry and unitarity and has already been employed successfully in the anomalous two-photon decays of π^0, η and η' [10]. Therein the one-loop contributions from the WZW Lagrangian were calculated and unitarity corrections beyond one loop were included by employing a coupled channel Bethe-Salpeter equation which satisfies unitarity constraints and generates vector mesons from composite states of pseudoscalar mesons. Although being similar in spirit to the complete vector meson dominance picture, this approach clearly distinguishes between the exchange of either one or two vector mesons. It turns out that for the two-photon decays the exchange of one vector meson is the dominant contribution, whereas the simultaneous exchange of two vector mesons is suppressed. This is in contradistinction to complete vector meson dominance where the coupling of photons to pseudoscalar mesons is always mediated by vector mesons.

The purpose of the present work is to extend this approach to the decays $\eta, \eta' \to \pi^+\pi^-\gamma$. We will first perform a complete one-loop calculation including all counter terms of unnatural parity up to chiral order p^6 and with the η' as a dynamical degree of freedom, but without employing large N_c counting rules. As we will show explicitly, the inclusion of the massive η' state does not lead to a renormalization of the WZW Lagrangian and therefore satisfies constraints from the anomalous Ward identities. Unitarity corrections and final state interactions are then appended within a coupled channel analysis which can be easily matched to the ChPT result.

The importance of resonance exchange for these decays can be studied without including vector mesons explicitly in the effective Lagrangian. Moreover, we will critically examine the issue of η-η' mixing for these decays.

This work is organized as follows. In the next section, the complete one-loop calculation of the decays is performed. The inclusion of unitarity corrections beyond one-loop is outlined in Sec. 3 and numerical results are presented in Sec. 4 along with a comparison with experimental data. Sec. 5 contains our conclusions.

2 One-loop calculation

The decays $\eta, \eta' \to \pi^+\pi^-\gamma$ arise from the unnatural parity part of the effective Lagrangian which collects the terms that are proportional to the tensor $\epsilon_{\mu\nu\alpha\beta}$. Within the effective theory the chiral anomalies of the underlying QCD Lagrangian are accounted for by the WZW term [1, 2, 11] [3]

$$S_{WZW}(U,v) = \int d^4x \mathcal{L}_{WZW} = -\frac{i}{80\pi^2}\int_{M_5}\langle\Sigma^5\rangle - \frac{i}{16\pi^2}\int_{M_4} W(U,v) \tag{1}$$

where

$$W(U,v) = i\left\langle U\, dU^\dagger U\, dU^\dagger U\, dU^\dagger v - U^\dagger dU\, U^\dagger dU\, U^\dagger dU\, v\right\rangle \tag{2}$$

with $\Sigma = U^\dagger dU$ and for the number of colors we set $N_c = 3$. The matrix valued field $U = \exp\{i\sqrt{2}\phi/f\}$ contains the Goldstone boson octet (π, K, η_8) and the singlet field η_0, where f is the pseudoscalar decay constant in the chiral limit. The expression $\langle\ldots\rangle$ denotes the trace in flavor space and we have displayed only the pieces of the Lagrangian relevant for the present work. We utilized, furthermore, the differential form notation

$$v = dx^\mu v_\mu, \qquad d = dx^\mu \partial_\mu \tag{3}$$

with the Grassmann variables dx^μ which yield the volume element $dx^\mu dx^\nu dx^\alpha dx^\beta = \epsilon^{\mu\nu\alpha\beta} d^4x$. In the second integral Minkowskian space M_4 is extended to a five-dimensional manifold M_5 and the U fields are functions on M_5, *cf.* [2, 11] for details. The external vector field $v = -eQA$ describes the coupling of the photon field $A = dx^\mu A_\mu$ to the mesons with $Q = \frac{1}{3}\mathrm{diag}(2,-1,-1)$ being the charge matrix of the light quarks.

In addition to the WZW anomaly action there is one more term of unnatural parity at fourth chiral order contributing to $\eta' \to \pi^+\pi^-\gamma$ at leading order and to the η decay via mixing at next-to-leading order $\mathcal{O}(p^6)$. This gauge invariant term arises due to the extension to the $U(3)$ framework and reads

$$d^4x\mathcal{L}^{(4)}_{ct} = i\, W_3\left\langle dU\, dU^\dagger dv + dU^\dagger dU\, dv\right\rangle \ , \tag{4}$$

where W_3 is a function of η_0, $W_3(\eta_0/f)$. The potential W_3 can be expanded in the singlet field with coefficients $w_3^{(j)}$ that are not fixed by chiral symmetry, while parity conservation implies that W_3 is an odd function of η_0.

At the tree level the contributing diagram is depicted in Fig. 1 with P symbolizing either an η or η'. Expanding U in Eqs. (1) and (4) in terms of ϕ yields the tree level vertex

[3] Note that for our purposes we can safely set the singlet axial vector field $\langle a_\mu\rangle$ and the derivative of the QCD vacuum angle, $\partial_\mu\theta$, to zero in S_{WZW} which enables us to work with the renormalization group invariant form of the anomaly.

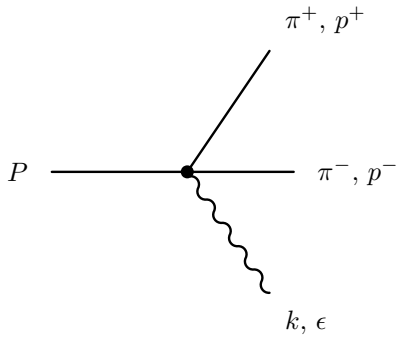

Figure 1: Tree diagram of the decay $P \to \pi^+\pi^-\gamma$, where p^+ and p^- denote the momenta of the outgoing pions. The momentum and the polarization of the photon are indicated by k and ϵ, respectively.

$$\begin{aligned} d^4x\mathcal{L}_{\rm WZW} &= \frac{i\sqrt{2}}{4\pi^2 f^3}\,\langle d\phi\, d\phi\, d\phi\, v\rangle + \dots\,, \\ d^4x\mathcal{L}^{(4)}_{ct} &= w_3^{(1)}\frac{4i}{f^3}\eta_0\,\langle d\phi\, d\phi\, dv\rangle + \dots\,. \end{aligned} \tag{5}$$

From these terms we can derive the tree level amplitude

$$\mathcal{A}^{(tree)}(P \to \pi^+\pi^-\gamma) = -ek_\mu\epsilon_\nu p^+_\alpha p^-_\beta \epsilon^{\mu\nu\alpha\beta}\frac{1}{4\pi^2 f^3}\alpha_P^{(tree)} \tag{6}$$

with

$$\alpha_\eta^{(tree)} = \frac{1}{\sqrt{3}}\,, \qquad\qquad \alpha_{\eta'}^{(tree)} = \sqrt{\frac{2}{3}} - 16\pi^2 w_3^{(1)}\,, \tag{7}$$

and $w_3^{(1)}$ is the coefficient of the leading term in W_3.

2.1 One-loop diagrams

There are four different topologies of one-loop graphs contributing to the $\pi^+\pi^-\gamma$ decays. We start with the discussion of the tadpole diagram shown in Fig. 2. The pertinent terms from

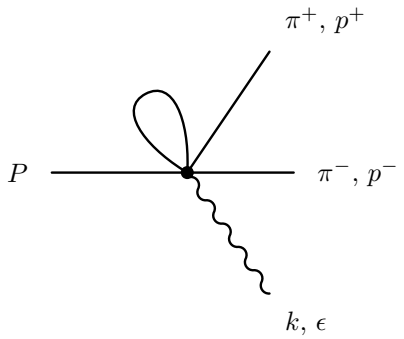

Figure 2: Tadpole diagram which contributes to $P \to \pi^+\pi^-\gamma$.

both the WZW and the unnatural parity Lagrangian are

$$\begin{aligned} d^4x\mathcal{L}_{\rm WZW} &= -\frac{i\sqrt{2}}{24\pi^2 f^5}\big\langle(\tfrac{1}{2}\phi[\phi\,,d\phi][d\phi\,,d\phi]+d\phi[d\phi\,,\phi[\phi\,,d\phi]] \\ &\qquad +[[d\phi\,,d\phi]d\phi\,,\phi^2]+\tfrac{3}{2}\phi[\phi\,,[d\phi\,,d\phi]d\phi])\,v\big\rangle+\dots\,, \\ d^4x\mathcal{L}^{(4)}_{ct} &= w_3^{(1)}\frac{2i}{3f^5}\eta_0\,\langle([\phi\,,d\phi][\phi\,,d\phi]-[\phi\,,[\phi\,,[d\phi\,,d\phi]]])\,dv\rangle\,, \\ &\quad + w_3^{(3)}\frac{4i}{f^5}\eta_0^3\,\langle d\phi\,d\phi\,dv\rangle+\dots\,. \end{aligned} \tag{8}$$

The $w_3^{(3)}$-term yields an η' tadpole which—strictly speaking—spoils the chiral counting scheme, as it contributes at fourth chiral order. However, the η' tadpole does not contain any infrared physics and can be absorbed completely into the low-energy constants (LECs) of the effective Lagrangian, as it is neither a function of the Goldstone boson masses nor of the external momenta, it is just a constant. This is consistent with the fact that in infrared regularization the η' tadpole vanishes, whereas the tadpoles for the Goldstone boson octet remain unaltered. By defining

$$w_3^{(1)} = w_3^{(1)r} - w_3^{(3)}\Delta_{\eta'}/f^2 \tag{9}$$

the η' tadpole is compensated by the second term in Eq. (9) and the chiral counting scheme is restored without renormalizing the WZW Lagrangian. The expression Δ_ϕ symbolizes the finite part of the tadpole integral

$$\Delta_\phi = \left(\int\frac{d^dl}{(2\pi)^d}\frac{i}{l^2-m_\phi^2+i\varepsilon}\right)_{\textit{finite}} = \frac{m_\phi^2}{16\pi^2}\,\ln\frac{m_\phi^2}{\mu^2} \tag{10}$$

with μ being the scale introduced in dimensional regularization. In the present work we are only concerned with the finite pieces of the diagrams and neglect the divergent portions throughout. Note that there are further contributions from one-loop graphs and counter terms which require a renormalization of $w_3^{(1)}$ as will be discussed below.

The remaining contributions in Eq. (8) to the amplitudes involve only Goldstone boson tadpoles and are thus of next-to-leading order

$$\mathcal{A}^{(tad)}(P\to\pi^+\pi^-\gamma) = -ek_\mu\epsilon_\nu p_\alpha^+ p_\beta^-\epsilon^{\mu\nu\alpha\beta}\frac{1}{4\pi^2 f^5}\left(\beta_P^{(tad),\pi}\Delta_\pi+\beta_P^{(tad),K}\Delta_K\right) \tag{11}$$

with

$$\begin{aligned} \beta_\eta^{(tad),\pi} &= -\frac{5}{3\sqrt{3}}\,, & \beta_{\eta'}^{(tad),\pi} &= -\frac{5}{3}\left(\sqrt{\frac{2}{3}}-16\pi^2 w_3^{(1)r}\right)\,, \\ \beta_\eta^{(tad),K} &= -\frac{4}{3\sqrt{3}}\,, & \beta_{\eta'}^{(tad),K} &= -\frac{5}{6}\left(\sqrt{\frac{2}{3}}-16\pi^2 w_3^{(1)r}\right)\,. \end{aligned} \tag{12}$$

Note that we have replaced the coefficient $w_3^{(1)}$ by the renormalized coupling $w_3^{(1)r}$ which is consistent at the one-loop level.

The loop graph in Fig. 3a has a four-meson vertex from the lowest order Lagrangian $\mathcal{L}^{(0+2)}$ of natural parity

$$\begin{aligned} \mathcal{L}^{(0+2)} &= \frac{f^2}{4}\left\langle D_\mu U^\dagger D^\mu U\right\rangle+\dots = \frac{1}{12f^2}\,\langle[\phi\,,\partial_\mu\phi][\phi\,,\partial^\mu\phi]\rangle+\dots\,, \\ D_\mu U &= \partial_\mu U + i[U,v_\mu]\,, \end{aligned} \tag{13}$$

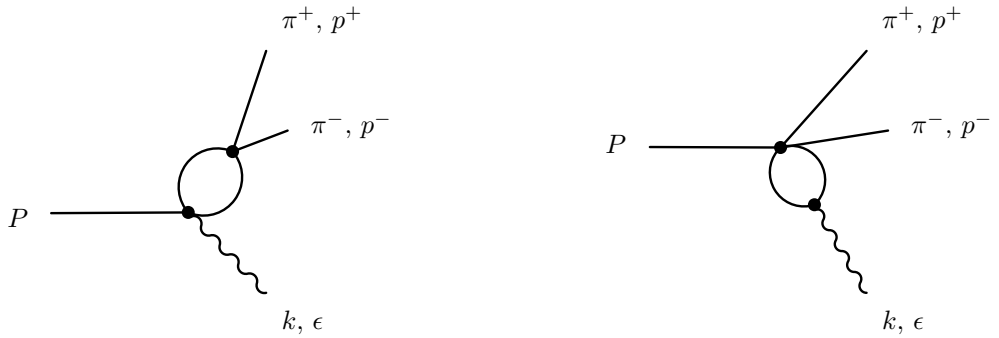

Figure 3: One-loop diagrams contributing to $P \to \pi^+\pi^-\gamma$.

which yields the amplitudes

$$\mathcal{A}^{(a)}(P \to \pi^+\pi^-\gamma) = -ek_\mu \epsilon_\nu p_\alpha^+ p_\beta^- \epsilon^{\mu\nu\alpha\beta} \frac{1}{4\pi^2 f^5} \Big(\beta_P^{(a),\pi} I_1(m_\pi^2; s_{+-}) + \beta_P^{(a),K} I_1(m_K^2; s_{+-}) \Big) \tag{14}$$

with $s_{+-} = (p^+ + p^-)^2$. The integral I_1 is defined by

$$I_1(m^2; p^2) = \frac{2}{3} \Big(\frac{1}{2}\Delta + (m^2 - \frac{p^2}{4}) G_{mm}(p^2) + \frac{1}{96\pi^2}(p^2 - 6m^2) \Big), \tag{15}$$

where G is the finite part of the scalar one-loop integral

$$\begin{aligned} G_{m\bar{m}}(p^2) &= \left(\int \frac{d^d l}{(2\pi)^d} \, \frac{i}{(l^2 - m^2 + i\epsilon)((l-p)^2 - \bar{m}^2 + i\epsilon)} \right)_{finite} \\ &= \frac{1}{16\pi^2} \Bigg[-1 + \ln \frac{m\bar{m}}{\mu^2} + \frac{m^2 - \bar{m}^2}{p^2} \ln \frac{m}{\bar{m}} \\ &\qquad - \frac{2\sqrt{\lambda_{m\bar{m}}(p^2)}}{p^2} \operatorname{artanh} \frac{\sqrt{\lambda_{m\bar{m}}(p^2)}}{(m+\bar{m})^2 - p^2} \Bigg], \end{aligned} \tag{16}$$

$$\lambda_{m\bar{m}}(p^2) = \big((m-\bar{m})^2 - p^2 \big) \big((m+\bar{m})^2 - p^2 \big).$$

The coefficients $\beta_P^{(a),\phi}$ read

$$\begin{aligned} \beta_\eta^{(a),\pi} &= \frac{1}{\sqrt{3}}, \qquad & \beta_{\eta'}^{(a),\pi} &= \sqrt{\frac{2}{3}} - 16\pi^2 w_3^{(1)r}, \\ \beta_\eta^{(a),K} &= \frac{2}{\sqrt{3}}, \qquad & \beta_{\eta'}^{(a),K} &= \frac{1}{\sqrt{6}} - 8\pi^2 w_3^{(1)r}. \end{aligned} \tag{17}$$

The diagram in Fig. 3b, on the other hand, involves the five-meson vertex of the WZW action

$$\frac{-i}{80\pi^2} \int_{x^5=0}^{x^5=1} \big\langle \Sigma^5 \big\rangle = \frac{\sqrt{2}}{20\pi^2 f^5} \, \langle \phi \, d\phi \, d\phi \, d\phi \, d\phi \rangle + \dots \, . \tag{18}$$

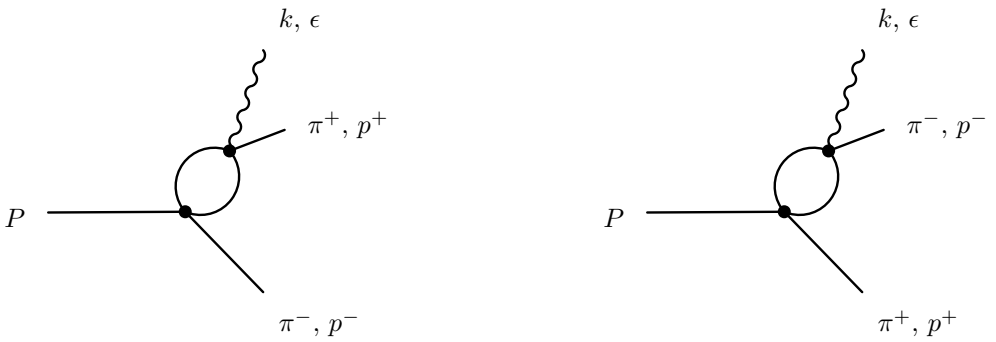

Figure 4: One-loop diagrams with an $\eta'\pi$ loop.

The singlet field η_0 does not contribute to the five-meson vertex and the η' is only involved via η-η' mixing which is of higher order in this framework. At $\mathcal{O}(p^6)$ the loop diagram in Fig. 3b thus yields a contribution only to the η decay

$$\mathcal{A}^{(b)}(P\to\pi^+\pi^-\gamma) = -ek_\mu\epsilon_\nu p^+_\alpha p^-_\beta \epsilon^{\mu\nu\alpha\beta}\frac{1}{4\pi^2 f^5}\beta_P^{(b)}\Delta_K \tag{19}$$

with

$$\beta_\eta^{(b)} = \sqrt{3}\,, \qquad \beta_{\eta'}^{(b)} = 0\,. \tag{20}$$

Two additional one-loop graphs which contribute at sixth chiral order are depicted in Fig. 4 and an analysis of the $\mathcal{O}(p^2)$ four-meson vertex shows that the only contribution to this diagram stems from

$$\mathcal{L}^{(0+2)} = V_1\left\langle D_\mu U^\dagger D^\mu U\right\rangle + \ldots = v_1^{(2)}\frac{2}{f^4}\eta_0^2\left\langle\partial_\mu\phi\partial^\mu\phi\right\rangle + \ldots \tag{21}$$

where $V_1(\eta_0/f) = f^2/4 + v_1^{(2)}\eta_0^2/f^2 + \ldots$. The fourth order vertex is given by Eq. (5) and we can readily calculate the amplitude

$$\mathcal{A}^{(c)}(P\to\pi^+\pi^-\gamma) = -ek_\mu\epsilon_\nu p^+_\alpha p^-_\beta \epsilon^{\mu\nu\alpha\beta}\frac{1}{4\pi^2 f^5}\;\beta_P^{(c)}\big(I_2(m_\pi^2,m_{\eta'}^2;s_{+\gamma}) + I_2(m_\pi^2,m_{\eta'}^2;s_{-\gamma})\big) \tag{22}$$

with $s_{+\gamma} = (p^+ + k)^2$ and $s_{-\gamma} = (p^- + k)^2$ and

$$\beta_\eta^{(c)} = 0\,, \qquad \beta_{\eta'}^{(c)} = -\frac{4v_1^{(2)}}{f^2}\left(\sqrt{\frac{2}{3}} - 16\pi^2 w_3^{(1)r}\right)\,, \tag{23}$$

where we have replaced again $w_3^{(1)}$ by $w_3^{(1)r}$ and neglected two-loop corrections. The finite part of the $\pi\eta'$ loop integral I_2 is given by

$$\begin{aligned} I_2(m_\pi^2,m_{\eta'}^2;p^2) =& \frac{1}{6p^2}\big\{-(p^2-(m_{\eta'}-m_\pi)^2)(p^2-(m_{\eta'}+m_\pi)^2)G_{m_\pi m_{\eta'}}(p^2) \\ &\qquad + (p^2 - m_{\eta'}^2 + m_\pi^2)\Delta_\pi + (p^2 + m_{\eta'}^2 - m_\pi^2)\Delta_{\eta'}\big\} \\ &+ \frac{1}{144\pi^2}(p^2 - 3m_\pi^2 - 3m_{\eta'}^2)\,. \end{aligned} \tag{24}$$

In order to maintain the matching between the chiral and the loop expansion of the amplitude, we have to absorb the contributions of $\mathcal{O}(p^4)$ in $\mathcal{A}^{(c)}$ into the leading order coupling $w_3^{(1)}$, Eq. (5). Expanding I_2 in terms of $\frac{p^2}{m_{\eta'}^2}$ and $\frac{m_\pi^2}{m_{\eta'}^2}$ yields

$$I_2(m_\pi^2, m_{\eta'}^2; p^2) = \frac{1}{2}\Big(\Delta_{\eta'} - \frac{m_{\eta'}^2}{32\pi^2}\Big)\Big(1 + \frac{m_\pi^2}{m_{\eta'}^2}\Big) - \frac{1}{6}\Big(\Delta_{\eta'} - \frac{m_{\eta'}^2}{96\pi^2}\Big)\frac{p^2}{m_{\eta'}^2} + \ldots \tag{25}$$

and the renormalization may be accomplished by modifying Eq. (9) according to

$$w_3^{(1)} = w_3^{(1)r} - w_3^{(3)}\frac{\Delta_{\eta'}}{f^2} - \frac{v_1^{(2)}}{4\pi^2 f^4}\left(\sqrt{\frac{2}{3}} - 16\pi^2 w_3^{(1)r}\right)\left(\Delta_{\eta'} - \frac{m_{\eta'}^2}{32\pi^2}\right), \tag{26}$$

where we replaced $w_3^{(1)}$ by $w_3^{(1)r}$ in the last term of Eq. (26). After this renormalization, we work with the subtracted integral

$$\hat{I}_2(m_\pi^2, m_{\eta'}^2; p^2) = I_2(m_\pi^2, m_{\eta'}^2; p^2) - I_2(0, m_{\eta'}^2; 0) \tag{27}$$

which yields contributions to the amplitude of order p^6 and higher. Thus all one-loop contributions of $\mathcal{O}(p^4)$ can be absorbed into a redefinition of the low-energy constant $w_3^{(1)}$ and do not renormalize the WZW Lagrangian.

We now turn to the next-to-leading order chiral corrections from the decay constants, η-η' mixing and wave-function renormalization which are readily calculated from the formulae given in [12]. Replacing in the tree level result, Eq. (6), the decay constant in the chiral limit by the corresponding one-loop expression induces the following $\mathcal{O}(p^6)$ corrections to the decay amplitudes

$$\mathcal{A}^{(f)}(P \to \pi^+\pi^-\gamma) = -ek_\mu\epsilon_\nu p_\alpha^+ p_\beta^- \epsilon^{\mu\nu\alpha\beta}\frac{1}{4\pi^2 F_P F_\pi^2}\alpha_P^{(tree)}\left(\frac{\delta F_P}{F_P^2} + 2\frac{\delta F_\pi}{F_P^2}\right), \tag{28}$$

where the δF_P are defined by $F_P = f(1 + \delta F_P/f^2)$ with [12]

$$\begin{aligned}
\delta F_\pi &= 4\beta_4^{(0)}(2m_K^2 + m_\pi^2) + 4\beta_5^{(0)}m_\pi^2 - \Delta_\pi - \frac{1}{2}\Delta_K\,,\\
\delta F_\eta &= 4\beta_4^{(0)}(2m_K^2 + m_\pi^2) + 4\beta_5^{(0)}m_\eta^2 - \frac{3}{2}\Delta_K\,,\\
\delta F_{\eta'} &= 4(2m_K^2 + m_\pi^2)\big(\beta_4^{(0)} + \frac{1}{3}\beta_5^{(0)} - 3\beta_{17}^{(0)} + \beta_{18}^{(0)} + \beta_{46}^{(0)} + 3\beta_{47}^{(0)} - \beta_{53}^{(0)} - \sqrt{\frac{3}{2}}\beta_{52}^{(1)}\big)\,.
\end{aligned} \tag{29}$$

In the case of the η' we employed the QCD renormalization scale invariant expression $F_{\eta'}$ which is derived from the singlet axial-vector matrix element of the η' and the $\beta_i^{(0)}$ are couplings of the natural parity part of the Lagrangian at fourth chiral order, see [10, 12] for details.

Wave-function renormalization for the external particles and η-η' mixing yield

$$\mathcal{A}^{(Z)}(P \to \pi^+\pi^-\gamma) = -ek_\mu\epsilon_\nu p_\alpha^+ p_\beta^- \epsilon^{\mu\nu\alpha\beta}\frac{1}{4\pi^2 F_P F_\pi^2}\beta_P^{(Z)} \tag{30}$$

with

$$\begin{aligned}
\beta_\eta^{(Z)} &= \alpha_\eta^{(tree)}\Big(R_{8\eta}^{(2)} + 2R_\pi^{(2)}\Big) + \alpha_{\eta'}^{(tree)}R_{0\eta}^{(2)}\,,\\
\beta_{\eta'}^{(Z)} &= \alpha_\eta^{(tree)}R_{8\eta'}^{(2)} + \alpha_{\eta'}^{(tree)}\Big(R_{0\eta'}^{(2)} + 2R_\pi^{(2)}\Big)\,,
\end{aligned} \tag{31}$$

and the $R^{(2)}$ can be found in [12].

2.2 Counter terms at $\mathcal{O}(p^6)$

The full set of contributing contact terms of unnatural parity at order p^6 in the $U(3)$ framework is presented in App. A. Expanding both the potentials and U in the meson fields one obtains (Eqs. (A.3), (A.5))

$$\begin{aligned}
d^4x\mathcal{L}_{ct}^{(6)} \;=\; & i\,\bar{w}_7^{(0)}\,\frac{8\sqrt{2}}{f^3}\,\langle\{\chi\,,\phi\}(\{d\phi\,d\phi\,,dv\}+2d\phi\,dv\,d\phi)\rangle \\
& + i\,\bar{w}_8^{(0)}\,\frac{32\sqrt{2}}{f^3}\,\langle\chi\,\phi\rangle\,\langle d\phi\,d\phi\,dv\rangle - \,i\,\bar{w}_9^{(0)}\,\frac{16\sqrt{6}}{f^3}\,\eta_0\,\langle\{\chi\,,d\phi\}[d\phi\,,dv]\rangle \\
& - i\,\bar{w}_{10}^{(0)}\,\frac{16\sqrt{6}}{f^3}\,\eta_0\,\langle\chi\rangle\,\langle d\phi\,d\phi\,dv\rangle \\
& - i\,\bar{w}_{11}^{(0)}\,\frac{16\sqrt{2}}{f^3}\,\big\langle(\partial^\lambda d\phi\,d\phi\,\partial_\lambda\phi+\partial_\lambda\phi\,d\phi\,\partial^\lambda d\phi)\,dv\big\rangle \\
& - i\,\bar{w}_{12}^{(0)}\,\frac{16\sqrt{2}}{f^3}\,\big\langle(\partial^\lambda d\phi\,\partial_\lambda\phi\,d\phi+d\phi\,\partial_\lambda\phi\,\partial^\lambda d\phi)\,dv\big\rangle \\
& - i\,\bar{w}_{13}^{(0)}\,\frac{16\sqrt{2}}{f^3}\,\langle d\phi\rangle\,\big\langle[\partial^\lambda d\phi\,,\partial_\lambda\phi]\,dv\big\rangle - \,i\,\bar{w}_{14}^{(0)}\,\frac{16\sqrt{2}}{f^3}\,\langle\partial_\lambda\phi\rangle\,\big\langle[\partial^\lambda d\phi\,,d\phi]\,dv\big\rangle\;. \qquad (32)
\end{aligned}$$

The first four terms contain the quark mass matrix $\mathcal{M}=\mathrm{diag}\,(\hat{m},\hat{m},m_s)$, $\hat{m}=m_u=m_d$, which enters in the combination $\chi=2B\mathcal{M}$ with $B=-\langle 0|\,\bar{q}q\,|0\rangle/f^2$ being the order parameter of the spontaneous symmetry violation, whereas the terms $\bar{w}_{11},\ldots,\bar{w}_{14}$ arise from the counter terms with five derivatives, since the external vector field counts as order p. The resulting counter term contributions to the decay amplitudes read

$$\mathcal{A}^{(ct)}(P\to\pi^+\pi^-\gamma)=-ek_\mu\epsilon_\nu p_\alpha^+ p_\beta^-\epsilon^{\mu\nu\alpha\beta}\frac{1}{4\pi^2 f^3}\;\beta_P^{(ct)} \qquad (33)$$

with

$$\begin{aligned}
\beta_\eta^{(ct)} &= \frac{64\pi^2}{\sqrt{3}}\Big\{-4\bar{w}_7^{(0)}m_\pi^2+8\bar{w}_8^{(0)}(m_K^2-m_\pi^2) \\
&\qquad +\bar{w}_{11}^{(0)}(m_\eta^2+2s_{+-}-2m_\pi^2)+\bar{w}_{12}^{(0)}(s_{+-}-2m_\pi^2)\Big\}\,, \\
\beta_{\eta'}^{(ct)} &= 32\pi^2\sqrt{\frac{2}{3}}\Big\{8(-\bar{w}_7^{(0)}+3\bar{w}_9^{(0)})m_\pi^2+(4\bar{w}_8^{(0)}+6\bar{w}_{10}^{(0)})(2m_K^2+m_\pi^2) \\
&\qquad +2\bar{w}_{11}^{(0)}(m_{\eta'}^2+2s_{+-}-2m_\pi^2)+3\bar{w}_{14}^{(0)}(m_{\eta'}^2+s_{+-}) \\
&\qquad +2(\bar{w}_{12}^{(0)}+3\bar{w}_{13}^{(0)})(s_{+-}-2m_\pi^2)\Big\}\;. \qquad (34)
\end{aligned}$$

The $\bar{w}_i^{(0)}$ are understood to be the finite parts of the coupling constants in the Lagrangian of sixth chiral order. Within $SU(3)$ ChPT the absorption of divergences from one-loop diagrams into the LECs of the $\mathcal{O}(p^6)$ Lagrangian has been discussed in [3]. For the numerical analysis it is convenient to decompose the $\beta_P^{(ct)}$ as follows,

$$\beta_\eta^{(ct)}=\frac{64\pi^2}{\sqrt{3}}\big(\bar{w}_\eta^{(m)}+\bar{w}_\eta^{(s)}s_{+-}\big) \qquad (35)$$

with

$$\bar{w}_\eta^{(m)} = (-4\bar{w}_7^{(0)} - 2\bar{w}_{11}^{(0)} - 2\bar{w}_{12}^{(0)})m_\pi^2 + 8\bar{w}_8^{(0)}(m_K^2 - m_\pi^2) + \bar{w}_{11}^{(0)} m_\eta^2\,,$$
$$\bar{w}_\eta^{(s)} = 2\bar{w}_{11}^{(0)} + \bar{w}_{12}^{(0)}\ , \tag{36}$$

and

$$\beta_{\eta'}^{(ct)} = 32\pi^2\sqrt{\frac{2}{3}}\big(\bar{w}_{\eta'}^{(0)} m_{\eta'}^2 + \bar{w}_{\eta'}^{(m)} + \bar{w}_{\eta'}^{(s)} s_{+-}\big) \tag{37}$$

with

$$\bar{w}_{\eta'}^{(0)} = 2\bar{w}_{11}^{(0)} + 3\bar{w}_{14}^{(0)}$$
$$\bar{w}_{\eta'}^{(m)} = -4(2\bar{w}_7^{(0)} - 6\bar{w}_9^{(0)} + \bar{w}_{11}^{(0)} + \bar{w}_{12}^{(0)} + 3\bar{w}_{13}^{(0)})m_\pi^2 + (4\bar{w}_8^{(0)} + 6\bar{w}_{10}^{(0)})(2m_K^2 + m_\pi^2)\,,$$
$$\bar{w}_{\eta'}^{(s)} = 4\bar{w}_{11}^{(0)} + 2\bar{w}_{12}^{(0)} + 6\bar{w}_{13}^{(0)} + 3\bar{w}_{14}^{(0)}\ . \tag{38}$$

The $\bar{w}_{\eta'}^{(0)}$ piece in $\beta_{\eta'}^{(ct)}$ can be absorbed into $w_3^{(1)}$

$$w_3^{(1)} = w_3^{(1)r} + \frac{1}{16\pi^2}\bar{w}_{\eta'}^{(0)} m_{\eta'}^2 - \dots\ , \tag{39}$$

where the ellipsis denotes the renormalization of the one-loop graphs given in Eq. (26) and in the following we employ the redefined value for $\beta_{\eta'}^{(ct)}$ after renormalization, $\beta_{\eta'}^{(ct)} = 32\pi^2\sqrt{\frac{2}{3}}\big(\bar{w}_{\eta'}^{(m)} + \bar{w}_{\eta'}^{(s)} s_{+-}\big)$, without changing the notation.

2.3 Full one-loop result

Summing up the contributions up to $\mathcal{O}(p^6)$ we arrive at

$$\mathcal{A}^{(1\text{-}loop)} = \mathcal{A}^{(tree)} + \mathcal{A}^{(tad)} + \mathcal{A}^{(a)} + \mathcal{A}^{(b)} + \mathcal{A}^{(c)} + \mathcal{A}^{(f)} + \mathcal{A}^{(Z)} + \mathcal{A}^{(ct)}\ . \tag{40}$$

The amplitude has the form

$$\mathcal{A}^{(1\text{-}loop)}(P \to \pi^+\pi^-\gamma) = -ek_\mu\epsilon_\nu p_\alpha^+ p_\beta^- \epsilon^{\mu\nu\alpha\beta}\frac{1}{4\pi^2 F_P F_\pi^2}\ \beta_P^{(1\text{-}loop)} \tag{41}$$

with

$$\beta_P^{(1\text{-}loop)} = \alpha_P^{(tree)}\left(1 + \frac{\delta F_P}{F_P^2} + 2\frac{\delta F_\pi}{F_P^2}\right) + \beta_P^{(tad),\pi}\,\frac{\Delta_\pi}{F_P^2} + (\beta_P^{(tad),K} + \beta_P^{(b)})\frac{\Delta_K}{F_P^2}$$
$$+\frac{\beta_P^{(a),\pi}}{F_P^2}\,I_1(m_\pi^2; s_{+-}) + \frac{\beta_P^{(a),K}}{F_P^2}\,I_1(m_K^2; s_{+-})$$
$$+\frac{\beta_P^{(c)}}{F_P^2}\left(\hat{I}_2(m_\pi^2, m_{\eta'}^2; s_{+\gamma}) + \hat{I}_2(m_\pi^2, m_{\eta'}^2; s_{-\gamma})\right) + \beta_P^{(Z)} + \beta_P^{(ct)}\,, \tag{42}$$

where we have replaced the decay constant in the chiral limit, f, by the decay constants F_P ($P = \eta, \eta'$) and F_π, Eq. (29), in such a way that the amplitude $\mathcal{A}^{(1\text{-}loop)}$ is accompanied by a factor $1/(F_P F_\pi^2)$. Note that in $\alpha_P^{(tree)}$ the coefficient $w_3^{(1)}$ has been replaced by $w_3^{(1)r}$, in order

to account for the renormalization of the p^4 contributions from loop graphs and counter terms. For convenience we also show the explicit form of the $\beta_P^{(1\text{-}loop)}$

$$\begin{aligned}
\beta_\eta^{(1\text{-}loop)} &= \frac{1}{\sqrt{3}}\Bigg\{1+\frac{1}{F_\eta^2}\Bigg[4\sqrt{\frac{2}{3}}\left(\sqrt{\frac{2}{3}}-16\pi^2 w_3^{(1)r}\right)(m_K^2-m_\pi^2)\frac{\tilde{v}_2^{(1)}}{v_0^{(2)}} \\
&\qquad -3\,\Delta_\pi + I_1(m_\pi^2;s_{+-}) + 2I_1(m_K^2;s_{+-})\Bigg] + 64\pi^2\big(\bar{w}_\eta^{(m)}+\bar{w}_\eta^{(s)}s_{+-}\big)\Bigg\}, \\
\beta_{\eta'}^{(1\text{-}loop)} &= \left(\sqrt{\frac{2}{3}}-16\pi^2 w_3^{(1)r}\right)\Bigg\{1+\frac{1}{F_{\eta'}^2}\Bigg[4(2m_K^2+m_\pi^2)\Big(\beta_{46}^{(0)}+3\beta_{47}^{(0)}-\beta_{53}^{(0)}-\sqrt{\frac{3}{2}}\beta_{52}^{(1)}\Big) \\
&\qquad -3\Delta_\pi-\frac{3}{2}\Delta_K+I_1(m_\pi^2;s_{+-})+\frac{1}{2}I_1(m_K^2;s_{+-}) \\
&\qquad -4v_1^{(2)}\big(\hat{I}_2(m_\pi^2,m_{\eta'}^2;s_{+\gamma})+\hat{I}_2(m_\pi^2,m_{\eta'}^2;s_{-\gamma})\big)\Bigg]\Bigg\} \\
&\quad +\frac{4}{3}\sqrt{\frac{2}{3}}(m_K^2-m_\pi^2)\left(4\frac{\beta_{5,18}}{F_{\eta'}^2}-\frac{\tilde{v}_2^{(1)}}{v_0^{(2)}}\right)+32\pi^2\sqrt{\frac{2}{3}}\big(\bar{w}_{\eta'}^{(m)}+\bar{w}_{\eta'}^{(s)}s_{+-}\big)\,, \qquad (43)
\end{aligned}$$

where we have used the abbreviations

$$\begin{aligned}
\tilde{v}_2^{(1)} &= \tfrac{1}{4}f^2-\tfrac{1}{2}\sqrt{6}v_3^{(1)}\,, \\
\beta_{5,18} &= \beta_5^{(0)}+\tfrac{3}{2}\beta_{18}^{(0)}\,. \qquad (44)
\end{aligned}$$

This generalizes the result from [3] to the $U(3)$ framework with the η' as an explicit degree of freedom.

3 Generation of resonances

Resonances, in particular the $\rho(770)$, play an important role in the decays of η and η' into $\pi^+\pi^-\gamma$. We include them in the same way as for the two-photon decays in [10], *i.e.* by employing a coupled channel Bethe-Salpeter equation (BSE) which satisfies unitarity constraints and generates resonances dynamically by an infinite string of meson-meson rescattering processes. The scattering potential A is calculated from the contact interactions of the effective Lagrangian up to fourth chiral order and iterated in the coupled channel Bethe-Salpeter equation

$$T = [\mathbb{1} + A\cdot\tilde{G}]^{-1}\,A \qquad (45)$$

with a modified scalar loop integral

$$\tilde{G}_{m\bar{m}} = G_{m\bar{m}}(\mu) + a_{m\bar{m}}(\mu)\,, \qquad (46)$$

where G has been defined in Eq. (16) and a is a real constant chosen in such a way that the μ dependent pieces of G and a compensate. For a diagrammatic illustration of the BSE, see Fig. 5. The resulting T matrix describes accurately the experimental phase shifts in both the s and p wave channels [10, 13].

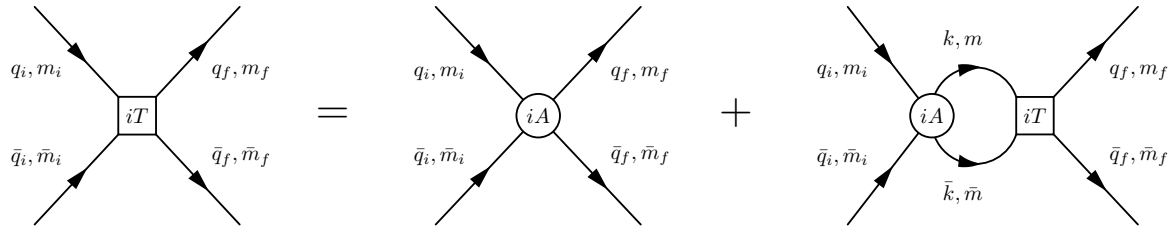

Figure 5: Diagrammatic Bethe-Salpeter equation for meson-meson rescattering.

In order to implement the non-perturbative summation of loop graphs covered by the BSE in the decay processes under consideration, we treat the BSE T matrix as an effective vertex for meson-meson scattering. The pertinent diagrams are shown in Fig. 6 and an analysis of the remaining loop integrations confirms that—as in the case of the two-photon decays—only the p wave part of T contributes.

There is, however, one difference to the two-photon decays. Whereas for the process $P \to \gamma^{(*)}\gamma^{(*)}$ the contributions of the coupled channels were at least of two-loop order, the diagrams (a) and (c) in Fig. 6 incorporate also one-loop contributions, since $T = A$ at lowest order. In order to avoid double counting, we omit those one-loop contributions from the last section which are already covered by the coupled channel calculation. Since the coupled channel diagrams (a) and (c) exactly reproduce the one-loop results at lowest order, the next-to-leading order calculation is still complete.

The amplitude of Fig. 6a is given by

$$\mathcal{A}^{(CCa)}(P \to \gamma^{(*)}\gamma^{(*)}) = -ek_\mu \epsilon_\nu p_\alpha^+ p_\beta^- \epsilon^{\mu\nu\alpha\beta} \frac{1}{4\pi^2 f^3} {\sum_a}' \gamma_P^{(CCa),a}\ \tilde{I}_1(m_a^2; s_{+-})\ \hat{T}_p^{(a\to\pi^\pm)}(s_{+-}) \quad (47)$$

with

$$\begin{aligned}
\gamma_\eta^{(CCa),\pi^\pm} &= \gamma_\eta^{(CCa),K^\pm} = \frac{1}{6}\left[\sqrt{3} + \frac{4\sqrt{2}}{3}(m_K^2 - m_\pi^2)\frac{\tilde{v}_2^{(1)}}{v_0^{(2)}}\left(\sqrt{6} - 48\pi^2 w_3^{(1)r}\right)\right], \\
\gamma_\eta^{(CCa),K^0\bar{K}^0} &= -\frac{\sqrt{3}}{2}, \\
\gamma_{\eta'}^{(CCa),\pi^\pm} &= \gamma_{\eta'}^{(CCa),K^\pm} \\
&= \frac{1}{6}\left[\sqrt{6} - 48\pi^2 w_3^{(1)r} + \frac{4\sqrt{6}}{3}(m_K^2 - m_\pi^2)\left(4\frac{\beta_{5,18}}{F_{\eta'}^2} - \frac{\tilde{v}_2^{(1)}}{v_0^{(2)}}\right)\right], \\
\gamma_{\eta'}^{(CCa),K^0\bar{K}^0} &= -2\sqrt{\frac{2}{3}}(m_K^2 - m_\pi^2)\left(4\frac{\beta_{5,18}}{F_{\eta'}^2} - \frac{\tilde{v}_2^{(1)}}{v_0^{(2)}}\right) . \qquad (48)
\end{aligned}$$

The symbol $\sum'$ in Eq. (47) denotes summation over the meson pairs $\pi^+\pi^-$, K^+K^- and $K^0\bar{K}^0$ and $\hat{T}_p^{(a\to b)}$ is the p wave part of the BSE T matrix for scattering of a meson pair a into a meson pair b as defined in [10]. The loop integral $\tilde{I}_1$ is given by

$$\tilde{I}_1(m_\phi^2; p^2) = I_1(m_\phi^2; p^2) + C_\phi\ p^2 \quad (49)$$

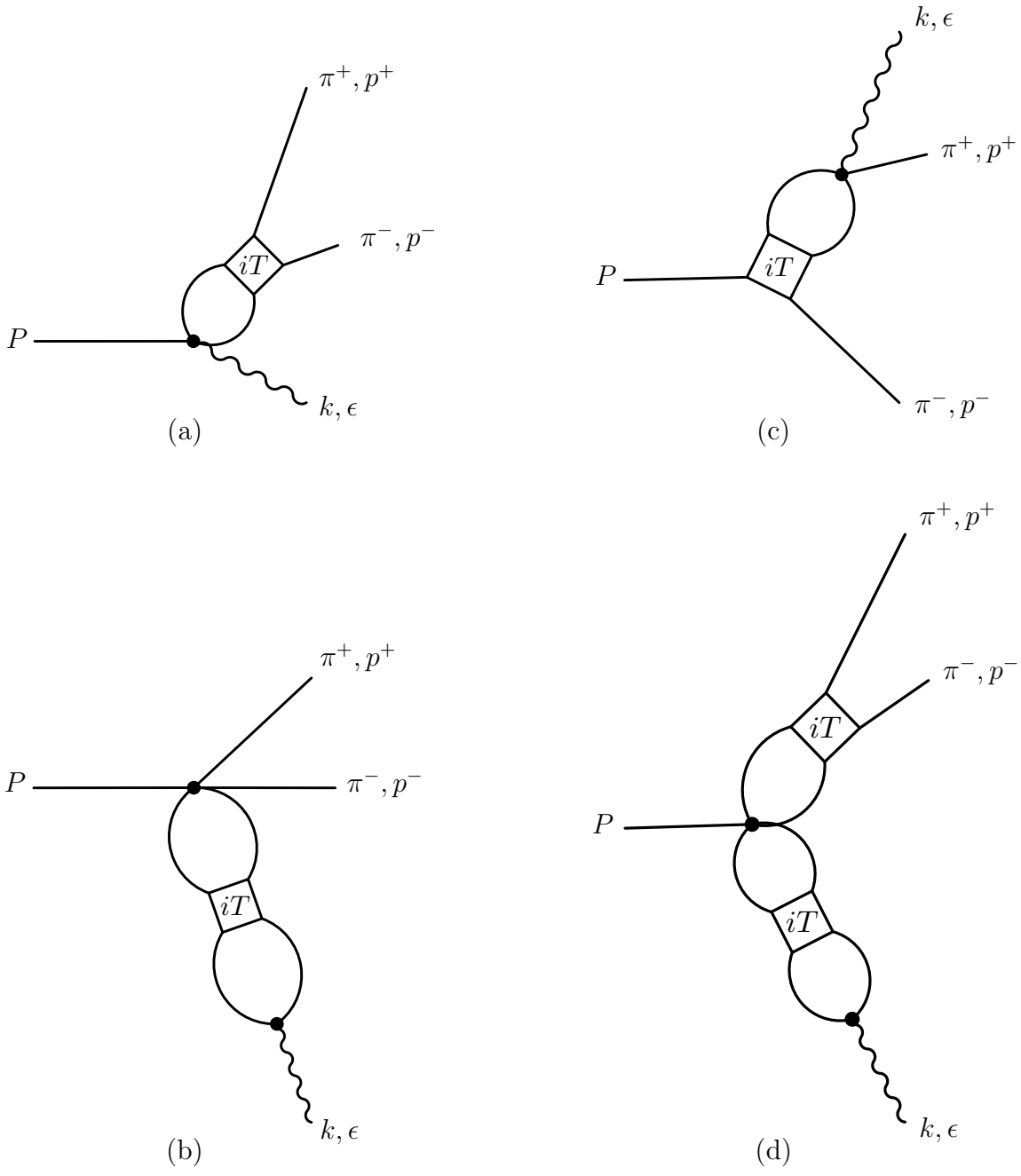

Figure 6: Set of meson-meson rescattering processes in the decay $P \to \pi^+\pi^-\gamma$ included in this approach. The crossed diagram of (c) is not shown.

with I_1 defined in Eq. (15) and in order to be in better agreement with experiment we make use of the freedom to take arbitrary values for the analytic pieces of the integrals which corresponds to a specific choice of counter term contributions.

The diagram in Fig. 6b yields the amplitude

$$\mathcal{A}^{(CCb)}(P\to\gamma^{(*)}\gamma^{(*)}) = -ek_\mu\epsilon_\nu p_\alpha^+ p_\beta^- \epsilon^{\mu\nu\alpha\beta}\frac{1}{4\pi^2 f^5}{\sum_a}' \gamma_P^{(CCb),a}\Delta_K \times\left[\hat{T}_p^{(a\to\pi^\pm)}(0)\ \Delta_\pi + \hat{T}_p^{(a\to K^\pm)}(0)\ \Delta_K\right], \quad (50)$$

where the coefficients $\gamma_P^{(CCb),a}$ are given by

$$\gamma_\eta^{(CCb),\pi^\pm} = \gamma_{\eta'}^{(CCb),\pi^\pm} = 0\,, \qquad \gamma_\eta^{(CCb),K^\pm} = -\gamma_\eta^{(CCb),K^0\bar{K}^0} = \frac{\sqrt{3}}{2}\,,$$
$$\gamma_{\eta'}^{(CCb),K^\pm} = -\gamma_{\eta'}^{(CCb),K^0\bar{K}^0} = 2\sqrt{\frac{2}{3}}(m_K^2-m_\pi^2)\left(4\frac{\beta_{5,18}}{F_{\eta'}^2} - \frac{\tilde{v}_2^{(1)}}{v_0^{(2)}}\right)\,. \quad (51)$$

The diagram in Fig. 6c involves the p wave scattering matrix for the two coupled channels $|\pi\eta\rangle$ and $|\pi\eta'\rangle$, so that the loop integral contains a pion and either an η or an η'.[4] The amplitude from Fig. 6c and the crossed diagram reads

$$\mathcal{A}^{(CCc)}(P\to\gamma^{(*)}\gamma^{(*)}) = -ek_\mu\epsilon_\nu p_\alpha^+ p_\beta^- \epsilon^{\mu\nu\alpha\beta}\frac{1}{4\pi^2 f^3} \times\frac{1}{2}\Bigg\{\frac{1}{\sqrt{3}}\big[I_2(m_\pi^2,m_\eta^2;s_{+\gamma})\ \hat{T}_p^{(P\pi^+\to\eta\pi^+)}(s_{+\gamma}) + I_2(m_\pi^2,m_\eta^2;s_{-\gamma})\ \hat{T}_p^{(P\pi^-\to\eta\pi^-)}(s_{-\gamma})\big] + \left(\sqrt{\frac{2}{3}} - 16\pi^2 w_3^{(1)r}\right)\big[\hat{I}_2(m_\pi^2,m_{\eta'}^2;s_{+\gamma})\ \hat{T}_p^{(P\pi^+\to\eta'\pi^+)}(s_{+\gamma}) + \hat{I}_2(m_\pi^2,m_{\eta'}^2;s_{-\gamma})\ \hat{T}_p^{(P\pi^-\to\eta'\pi^-)}(s_{-\gamma})\big]\Bigg\}, \quad (52)$$

and the integrals I_2 and $\hat{I}_2$ have been defined in Eq. (24) and Eq. (27), respectively.

We also consider the diagram with two coupled channels depicted in Fig. 6d. The pertinent amplitude reads

$$\mathcal{A}^{(2\,CC)}(P\to\gamma^{(*)}\gamma^{(*)}) = -ek_\mu\epsilon_\nu p_\alpha^+ p_\beta^- \epsilon^{\mu\nu\alpha\beta}\frac{1}{4\pi^2 f^5}{\sum_{a,b}}' \gamma_P^{(2\,CC),a,b} \times\tilde{I}_1(m_a^2;s_{+-})\ \hat{T}_p^{(a\to\pi^\pm)}(s_{+-})\ \Delta_b\big[\hat{T}_p^{(b\to\pi^\pm)}(0)\ \Delta_\pi + \hat{T}_p^{(b\to K^\pm)}(0)\ \Delta_K\big]\,. \quad (53)$$

[4]The (π,η) loop stems from the $\mathcal{O}(p^4)$ part of the scattering potential A and did thus not appear in the next-to-leading order calculation, where only the four-meson vertex of second chiral order was considered.

with coefficients $\gamma_P^{(2\,CC),a,b}$ symmetric under $a \leftrightarrow b$

$$\begin{aligned}
\gamma_\eta^{(2\,CC),\pi^\pm,K^\pm} &= -\gamma_\eta^{(2\,CC),\pi^\pm,K^0\bar{K}^0} = -\frac{1}{2}\gamma_\eta^{(2\,CC),K^\pm,K^0\bar{K}^0} = \frac{\sqrt{3}}{4}\,, \\
\gamma_{\eta'}^{(2\,CC),\pi^\pm,K^\pm} &= -\gamma_{\eta'}^{(2\,CC),\pi^\pm,K^0\bar{K}^0} = -\frac{1}{2}\gamma_{\eta'}^{(2\,CC),K^\pm,K^0\bar{K}^0} \\
&= \sqrt{\frac{2}{3}}(m_K^2 - m_\pi^2)\left(4\frac{\beta_{5,18}}{F_{\eta'}^2} - \frac{\tilde{v}_2^{(1)}}{v_0^{(2)}}\right)
\end{aligned} \tag{54}$$

and zero otherwise.

4 Numerical results

The spectra of the decays $\eta, \eta' \to \pi^+\pi^-\gamma$ have been measured with high statistics [4, 5, 9, 8] showing that the η' decay is clearly dominated by the ρ resonance. Therefore, the next-to-leading order calculation of Sec. 2 is insufficient to describe the η' decay and we will discuss the one-loop results only for the η decay. As a first estimate we use a set of parameters which is consistent with previous one-loop calculations in $U(3)$ ChPT [10, 12, 15]

$$\begin{aligned}
F_\pi &= 92.4\,\text{MeV}\,, \qquad F_\eta = 1.3F_\pi\,, \qquad F_{\eta'} = 1.1F_\pi\,, \\
\beta_5^{(0)} &= 1.4\cdot 10^{-3}\,, \qquad \tilde{v}_2^{(1)} = 1.2F_\pi^2/4,
\end{aligned} \tag{55}$$

while neglecting all other LECs including the coupling constants of the unnatural parity Lagrangian of sixth chiral order. For the regularization scale μ we use 1 GeV. The decay width turns out to be $\Gamma_\eta = 14.48$ eV which is by a factor of four smaller than the experimental value quoted by the Particle Data Group [14]

$$\Gamma_\eta = (56.1 \pm 5.4)\,\text{eV}\,. \tag{56}$$

A mixing parameter of $\tilde{v}_2^{(1)} = 0.5F_\pi^2/4$ corresponds to an even smaller decay width of $\Gamma_\eta = 8.59$ eV, whereas a value of $\tilde{v}_2^{(1)} = 1.5F_\pi^2/4$ results in $\Gamma_\eta = 17.47$ eV. Hence, for realistic values of the η-η' mixing parameter $\tilde{v}_2^{(1)}$, it is not possible to match the experimental decay width without including the contact terms of $\mathcal{O}(p^6)$.

However, both the photon spectrum and the partial width of the decay $\eta \to \pi^+\pi^-\gamma$ can be reproduced at next-to-leading order, if $\mathcal{O}(p^6)$ counter terms are included. But the choice of parameters is not unique, hence it is not possible to constrain the mixing parameter $\tilde{v}_2^{(1)}$ from a fit to the experimental data on the η decay, since variations in $\tilde{v}_2^{(1)}$ can be compensated by tuning the counter terms of unnatural parity; larger positive values of $\tilde{v}_2^{(1)}$, *e.g.*, require smaller counter term contributions. For consistency with previous one-loop calculations in $U(3)$ ChPT [10, 12, 15] we prefer to use a mixing parameter of $\tilde{v}_2^{(1)} = 1.2F_\pi^2/4$. At the one-loop level the constants $w_3^{(1)r}$ and $\bar{w}_\eta^{(m)}$ appear in a linear combination and thus cannot be fixed separately. In order to work with a minimum set of parameters, we set in the one-loop calculation $w_3^{(1)r}$ to zero and choose the combinations of counter terms Eq. (36) to be $\bar{w}_\eta^{(m)} = -0.31\cdot 10^{-3}$ and $\bar{w}_\eta^{(s)} = 12.9\cdot 10^{-3}\,\text{GeV}^{-2}$.

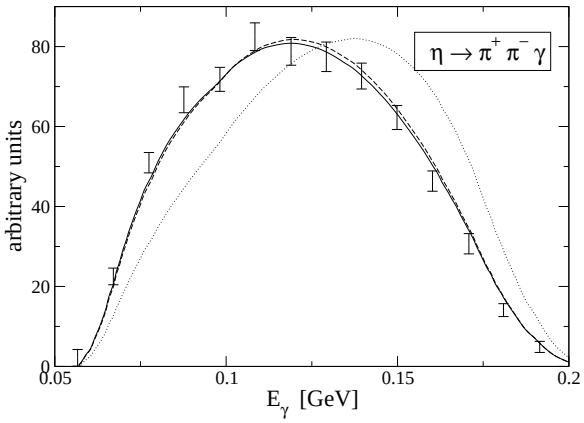

Figure 7: Photon spectrum resulting from the next-to-leading order calculation with p^6 counter terms (dashed) and from the full calculation including the coupled channels (solid). The dotted line corresponds to the simplest gauge invariant amplitude $\mathcal{A} \propto k_\mu \epsilon_\nu p_\alpha^+ p_\beta^- \epsilon^{\mu\nu\alpha\beta}$. The data are taken from [4].

The one-loop result is compared with experimental data from [4] in Fig. 7 and shows good agreement after accounting for the detection efficiencies. Good agreement with the similar experiment [5] is also achieved. It should be mentioned that the counter term contribution $\bar{w}_\eta^{(s)}$ yields an important contribution to the decay amplitude and dominates the one-loop corrections. This fact is a reflection of the tail of the ρ resonance in the perturbative expansion [3].

We now turn to the discussion of the coupled channel calculation. The computation includes the tree level graphs and all next-to-leading order corrections. In order to avoid double counting, the one-loop contributions which are already covered by the coupled channel diagrams in Figs.6a, c have been subtracted. The results are plotted in Figs. 7, 8 and compared with the experimental data. The agreement with the data is very good and shows that the important degrees of freedom are incorporated in our model. For consistency with previous calculations in this framework [10, 16], we have set the mixing parameter $\tilde{v}_2^{(1)}$ and the renormalized coupling constant $w_3^{(1)r}$ from the unnatural parity $\mathcal{O}(p^4)$ Lagrangian to zero. We furthermore neglect the unknown LEC $v_1^{(2)}$, in order to work with a minimal set of free parameters. For the fit of our results to the central experimental values of the partial decay widths, $\Gamma_\eta = 56.1$ eV and $\Gamma_{\eta'} = 59.6$ keV [14], respectively, we employ for the subtraction constant C_π in the outer loop integral with pions (Eq. (49)) the value $C_\pi(\mu = 1\,\mathrm{GeV}) = -1.42 \cdot 10^{-2}$ which is comparable in size with the one used in [10] ($C_\pi = -1/(6\pi^2) \approx -1.69 \cdot 10^{-2}$), while setting those for the other loops to zero. Since different sets of counter term contributions are summarized in C_π, the values of these subtraction constants may differ for the decays into $2\pi\gamma$ or two photons. The counter term contributions from the Lagrangian of sixth chiral order are needed to bring our results to better agreement with the shape of the experimental spectra. The values for the combinations of LECs in Eqs. (36) and (38) are

$$\begin{aligned} \bar{w}_\eta^{(m)} &= -2.21 \cdot 10^{-3}\,, \qquad & \bar{w}_\eta^{(s)} &= -9.50 \cdot 10^{-3}\,\mathrm{GeV}^{-2}\,, \\ \bar{w}_{\eta'}^{(m)} &= -6.90 \cdot 10^{-3}\,, \qquad & \bar{w}_{\eta'}^{(s)} &= 1.00 \cdot 10^{-3}\,\mathrm{GeV}^{-2}\,. \end{aligned} \tag{57}$$

It should be emphasized that the choice of parameters is not unique, since for $\eta, \eta' \to \pi^+\pi^-\gamma$

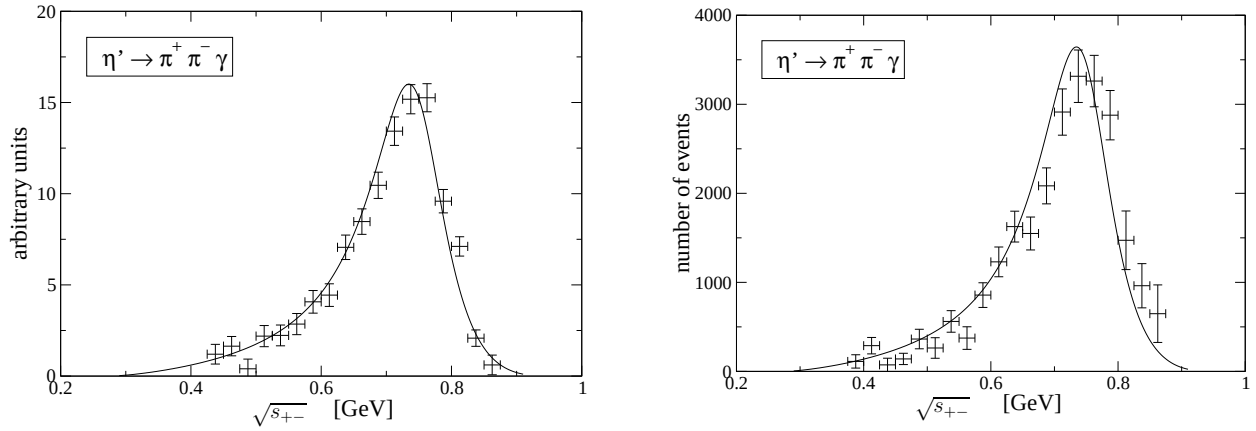

Figure 8: Invariant mass spectrum of the $\pi^+\pi^-$ system resulting from the full calculation. The curves are normalized to the integral of the experimental distribution. Data: left diagram [8], right diagram [9].

variations in one of the parameters may be compensated by the other ones. However, with the choice in Eq. (57) the remaining set of parameters is in agreement with previous work [10, 16].

In general, the values of the counter terms in the non-perturbative coupled channels approach differ from those in the one-loop calculation as already observed for the two-photon decays [10] and the hadronic decays of η and η' [16], since in the loopwise expansion the effects of resonances are hidden in the LECs, whereas they are generated dynamically in the non-perturbative approach.

In Fig. 9 we show the dependence of our results on the η-η' mixing parameter $\tilde{v}_2^{(1)}$. In both decays the heights of the spectra are reduced for increasing values of $\tilde{v}_2^{(1)}$ yielding smaller decay widths. As for the two-photon and hadronic decays, $\tilde{v}_2^{(1)} \approx 0$ is thus in better agreement with the data.

The results for different values of the LEC $w_3^{(1)r}$ are depicted in Fig. 10. When keeping $\tilde{v}_2^{(1)} = 0$, the η decay is not affected significantly. Similar to the two-photon decays negative values for $w_3^{(1)r}$ increase the ρ peak while positive values decrease it. Changes in $w_3^{(1)r}$ could in principle be compensated by altering the subtraction constant C_π in the loop integral $\tilde{I}_1$. The influence of $v_1^{(2)}$ on our results is rather small. Variations within a natural range for a coupling constant in the $\mathcal{O}(p^2)$ Lagrangian[5], $-3.0 \cdot 10^{-3}\,\mathrm{GeV}^2, \ldots, 3.0 \cdot 10^{-3}\,\mathrm{GeV}^2$, yield only slight corrections.

Finally, we compare the contributions of the different coupled channel diagrams in Fig. 6. From the plots in Fig. 11 we see that the amplitude for the pure $\pi^+\pi^-$ final state interaction, $\mathcal{A}^{(CCa)}$ (Eq. (47)), furnishes by far the dominant part. The diagrams which involve the five-meson vertex from the WZW Lagrangian (Fig. 6b, d) yield small corrections. This is in contradistinction to complete Vector Meson Dominance, where only these two diagrams are present. The contributions from the coupled channel diagram in Fig. 6c are almost negligible.

[5]The coefficients of $\langle \partial_\mu U^\dagger \partial^\mu U \rangle$ and $\langle U^\dagger \chi + \chi^\dagger U \rangle$ are $f^2/4 \approx F_\pi^2/4 \approx 2.22 \cdot 10^{-3}\,\mathrm{GeV}^2$, for comparison.

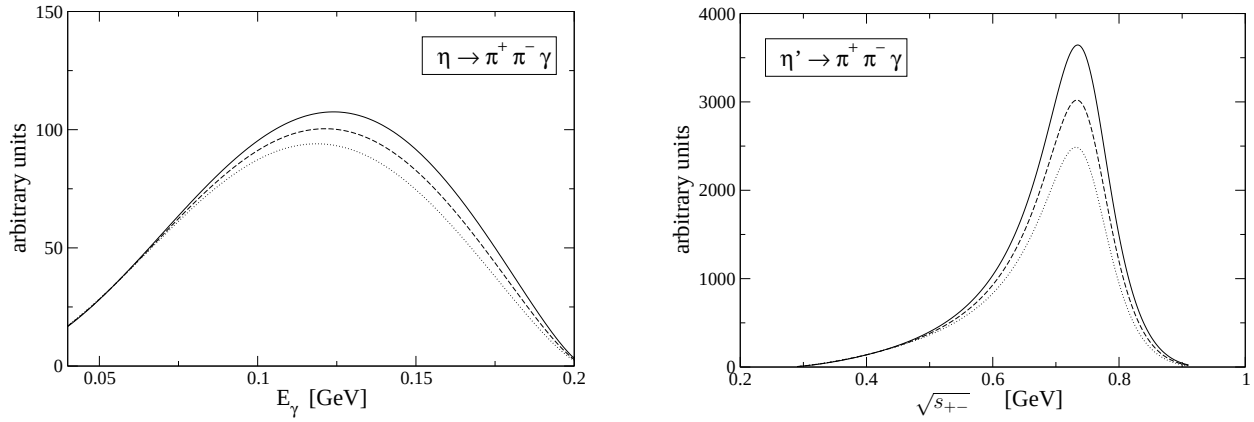

Figure 9: Dependence on the mixing parameter $\tilde{v}_2^{(1)}$: $\tilde{v}_2^{(1)} = 0$ (solid), $\tilde{v}_2^{(1)} = 0.6F_\pi^2/4$ (dashed), $\tilde{v}_2^{(1)} = 1.2F_\pi^2/4$ (dotted).

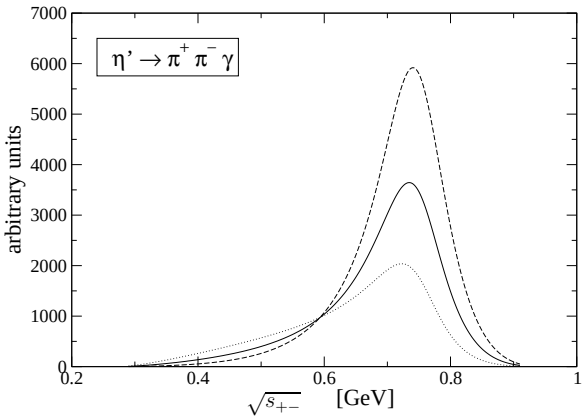

Figure 10: Dependence on the LEC $w_3^{(1)r}$: $w_3^{(1)r} = -2.0 \times 10^{-3}$ (dashed), $w_3^{(1)r} = 0$ (solid), $w_3^{(1)r} = 2.0 \times 10^{-3}$ (dotted).

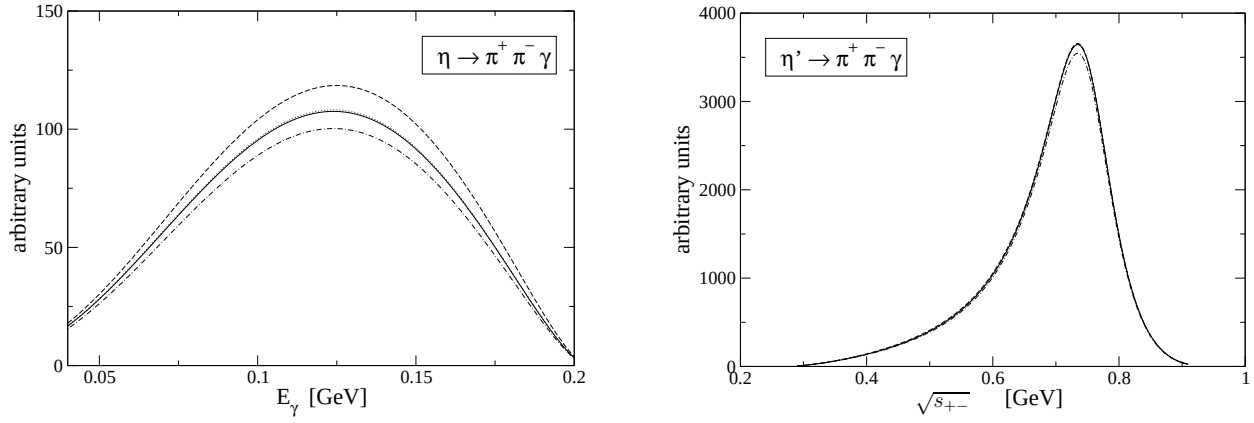

Figure 11: Comparison of the different coupled channel contributions in Fig. 6: Full result (solid), result without $\mathcal{A}^{(CCb)}$ (dashed), without $\mathcal{A}^{(CCc)}$ (dotted), without $\mathcal{A}^{(CCd)}$ (dot-dashed).

5 Conclusions

In this work, we have calculated the anomalous decays $\eta, \eta' \to \pi^+\pi^-\gamma$ within an approach that combines ChPT with a non-perturbative scheme based on coupled channels. This method satisfies unitarity constraints and generates vector mesons from composed states of pseudoscalar mesons without including them explicitly in the effective Lagrangian. It had recently been applied in the anomalous sector for the two-photon decays of π^0, η and η' and is now extended to the decays into $2\pi\gamma$.

We first performed a full one-loop calculation within the framework of chiral perturbation theory and without imposing large N_c counting rules. The presence of the massive state η' spoils the strict chiral counting scheme such that loop diagrams with an η' also contribute at fourth chiral order, *i.e.* at the same order as tree level contributions from the WZW Lagrangian. We have shown explicitly that these contributions can be absorbed into a non-anomalous contact interaction of unnatural parity, but they do not renormalize the WZW term so that the anomalous Ward identities are preserved.

If the counter terms of unnatural parity at subleading chiral order p^6 are omitted in the one-loop calculation, the results are in disagreement with the experimental decay widths. Taking η-η' mixing into account ameliorates the situation slightly for the η decay, but is still in contradiction to experiment. As a matter of fact, it is not possible to constrain η-η' mixing from the decay $\eta \to \pi^+\pi^-\gamma$. Moreover, one should keep in mind that mixing effects are of sixth chiral order, if large N_c counting rules are not employed, and enter at the same order as the neglected counter terms. The inclusion of contact interactions of sixth chiral order improves the situation for the η decay, whereas the results for the η' decay cannot be brought to agreement with experiment by adjusting the counter terms of sixth chiral order. This is due to the presence of vector mesons, which dominate the η' decay. While for the η decay only effects of the tail of the resonances contribute which can be treated perturbatively by absorbing them into the couplings of the effective Lagrangian, one must include unitarity effects via final state interactions in the η' decay.

The inclusion of the coupled channel formalism provides a framework which reproduces both the decay widths and the experimental dipion invariant-mass spectra of the η and η' decays while matching onto the results of ChPT. Our choice of parameters is consistent with that of the two-photon decays as discussed in [10] and provides a non-trivial check for our approach. It furthermore confirms that the inclusion of unitarity effects via the Bethe-Salpeter equation can be accomplished in the anomalous sector of QCD in a similar way as for the hadronic decays of η and η' [16]. Finally, we have shown that this method does not renormalize the WZW term and hence satisfies constraints from anomalous Ward identities.

6 Acknowledgements

We would like to thank Edisher Lipartia for useful discussions.

A $\mathcal{O}(p^6)$ Contact Terms in $P \to \pi^+\pi^-\gamma$

In this section we discuss the $\mathcal{O}(p^6)$ counter terms which contribute to η and η' decays into $\pi^+\pi^-\gamma$. We use the notation of [10] for the covariant derivative $D_\mu U$ and the field strength

tensors $\tilde{R}_{\mu\nu}$ and $\tilde{L}_{\mu\nu}$ of the right- and left-handed external fields, respectively, and make use of the following abbreviations:

$$\begin{aligned} \tilde{P}_{\mu\nu} &= U^\dagger \tilde{R}_{\mu\nu} U + \tilde{L}_{\mu\nu}\,, & \tilde{Q}_{\mu\nu} &= U^\dagger \tilde{R}_{\mu\nu} U - \tilde{L}_{\mu\nu}\,, \\ M &= U^\dagger \chi + \chi^\dagger U\,, & N &= U^\dagger \chi - \chi^\dagger U\,, \\ C_\mu &= U^\dagger D_\mu U\,, & E_{\mu\nu} &= U^\dagger D_\mu D_\nu U - (D_\mu D_\nu U)^\dagger U\,. \end{aligned} \tag{A.1}$$

These are the building blocks for the construction of the counter terms. Essentially, there are two types of counter terms; either they include the mass matrix $\mathcal{M} = \mathrm{diag}(\hat{m}, \hat{m}, m_s)$ or they contain two additional derivatives resulting in contributions to the decay amplitude proportional to s_{+-} which can be expressed in terms of the photon energy ω. In the $SU(3)$ framework the entire set of $\mathcal{O}(p^6)$ terms of unnatural parity has been presented in [17], but the inclusion of the singlet field η_0 induces additional structures. The mass terms may be written as

$$\begin{aligned} \mathcal{L}_\chi^{(6)} = \epsilon^{\mu\nu\alpha\beta}\Big\{ & \bar{W}_7 \left\langle N(\tilde{P}_{\mu\nu} C_\alpha C_\beta + C_\alpha C_\beta \tilde{P}_{\mu\nu} + 2 C_\alpha \tilde{P}_{\mu\nu} C_\beta) \right\rangle \\ & + \bar{W}_8 \left(\langle M C_\mu \rangle \left\langle C_\nu \tilde{Q}_{\alpha\beta} \right\rangle + \langle N \rangle \left\langle \tilde{P}_{\mu\nu} C_\alpha C_\beta \right\rangle \right) \\ & + \bar{W}_9 \left(\left\langle M(\tilde{Q}_{\mu\nu} C_\alpha + C_\alpha \tilde{Q}_{\mu\nu}) \right\rangle + \left\langle N(\tilde{P}_{\mu\nu} C_\alpha - C_\alpha \tilde{P}_{\mu\nu}) \right\rangle \right) \langle C_\beta \rangle \\ & + \bar{W}_{10} \langle M \rangle \left\langle \tilde{Q}_{\mu\nu} C_\alpha \right\rangle \langle C_\beta \rangle \Big\}\,, \end{aligned} \tag{A.2}$$

where the last two terms arise from the extension to $U(3)$. Expansion in the meson fields yields in the differential form notation of [11]

$$\begin{aligned} d^4x \mathcal{L}_{\chi,\,ct}^{(6)} \;=\; & i\,\bar{w}_7^{(0)}\,\frac{8\sqrt{2}}{f^3}\,\langle \{\chi\,,\phi\}(\{d\phi\,d\phi\,,dv\} + 2 d\phi\,dv\,d\phi)\rangle \\ & + i\,\bar{w}_8^{(0)}\,\frac{32\sqrt{2}}{f^3}\,\langle \chi\,\phi\rangle\,\langle d\phi\,d\phi\,dv\rangle - \,i\,\bar{w}_9^{(0)}\,\frac{16\sqrt{6}}{f^3}\,\eta_0\,\langle \{\chi\,,d\phi\}[d\phi\,,dv]\rangle \\ & - i\,\bar{w}_{10}^{(0)}\,\frac{16\sqrt{6}}{f^3}\,\eta_0\,\langle\chi\rangle\,\langle d\phi\,d\phi\,dv\rangle \end{aligned} \tag{A.3}$$

and we have integrated by parts in order to simplify the structures. The terms with five derivatives and one external field are

$$\begin{aligned} \mathcal{L}_\partial^{(6)} = \epsilon^{\mu\nu\alpha\beta}\Big\{ & \bar{W}_{11} \left\langle \tilde{P}_{\mu\nu} (E^\lambda{}_\alpha C_\beta C_\lambda - C_\lambda C_\beta E^\lambda{}_\alpha) \right\rangle \\ & + \bar{W}_{12} \left\langle \tilde{P}_{\mu\nu} (E^\lambda{}_\alpha C_\lambda C_\beta - C_\beta C_\lambda E^\lambda{}_\alpha) \right\rangle \\ & + \bar{W}_{13} \left\langle \tilde{P}_{\mu\nu} (E^\lambda{}_\alpha C_\lambda - C_\lambda E^\lambda{}_\alpha) \right\rangle \langle C_\beta \rangle \\ & + \bar{W}_{14} \left\langle \tilde{P}_{\mu\nu} (E^\lambda{}_\alpha C_\beta - C_\beta E^\lambda{}_\alpha) \right\rangle \langle C_\lambda \rangle \Big\} \end{aligned} \tag{A.4}$$

with $\bar{W}_{13}$ and $\bar{W}_{14}$ being only present in the $U(3)$ framework. Expansion in ϕ yields the vertices

$$\begin{aligned} d^4x\mathcal{L}^{(6)}_{\partial,\,ct} = &- i\,\bar{w}^{(0)}_{11}\,\frac{16\sqrt{2}}{f^3}\left\langle(\partial^\lambda d\phi\,d\phi\,\partial_\lambda\phi + \partial_\lambda\phi\,d\phi\,\partial^\lambda d\phi)\,dv\right\rangle \\ &- i\,\bar{w}^{(0)}_{12}\,\frac{16\sqrt{2}}{f^3}\left\langle(\partial^\lambda d\phi\,\partial_\lambda\phi\,d\phi + d\phi\,\partial_\lambda\phi\,\partial^\lambda d\phi)\,dv\right\rangle \\ &- i\,\bar{w}^{(0)}_{13}\,\frac{16\sqrt{2}}{f^3}\left\langle d\phi\right\rangle\left\langle[\partial^\lambda d\phi\,,\partial_\lambda\phi]\,dv\right\rangle \\ &- i\,\bar{w}^{(0)}_{14}\,\frac{16\sqrt{2}}{f^3}\left\langle\partial_\lambda\phi\right\rangle\left\langle[\partial^\lambda d\phi\,,d\phi]\,dv\right\rangle\ . \end{aligned} \tag{A.5}$$

References

[1] J. Wess and B. Zumino, Phys. Lett. **B37** (1971) 95

[2] E. Witten, Nucl. Phys. **B223** (1983) 422

[3] J. Bijnens, A. Bramon, and F. Cornet, Phys. Lett. **B237** (1990) 488

[4] M. Gormley et al., Phys. Rev. **D2** (1970) 501

[5] J. G. Layter et al., Phys. Rev. **D7** (1973) 2565

[6] B. R. Holstein, Phys. Scripta T99 (2002) 55

[7] E. P. Venugopal and B. R. Holstein, Phys. Rev. **D57** (1998) 4397

[8] Crystal Barrel Collab., A. Abele et al., Phys. Lett. **B402** (1997) 195

[9] GAMS-200 Collab., S. I. Bityukov et al., Z. Phys. **C50** (1991) 451

[10] B. Borasoy and R. Nißler, Eur. Phys. J. **A19** (2004) 367

[11] R. Kaiser and H. Leutwyler, Eur. Phys. J. **C17** (2000) 623

[12] N. Beisert and B. Borasoy, Eur. Phys. J. **A11** (2001) 329

[13] N. Beisert and B. Borasoy, Phys. Rev. **D67** (2003) 074007

[14] Particle Data Group, K. Hagiwara et al., Phys. Rev. D66 (2002) 010001

[15] N. Beisert and B. Borasoy, Nucl. Phys. **A705** (2002) 433

[16] N. Beisert and B. Borasoy, Nucl. Phys. **A716** (2003) 186

[17] D. Issler, Report SLAC-PUB-4943, 1990 (unpublished);
R. Akhoury and A. Alfakih, Ann. Phys. (N.Y.) **210** (1991) 81;
H. W. Fearing and S. Scherer, Phys. Rev. **D53** (1996) 315;
J. Bijnens, L. Girlanda and P. Talavera, Eur. Phys. J. **C23** (2002) 539;
T. Ebertshäuser, H. W. Fearing, S. Scherer, Phys. Rev. **D65** (2002) 054033